Application of chiral bag model to pion photoproduction

M. T. Jeong and Il-T. Cheon
Department of Physics, Yonsei University, Seoul 120-749, Korea
(Received 8 December 1988)

Scattering amplitudes for the pion photoproductions have been derived on the chiral bag model by taking into account pion cloud effects, pion-pole term, and antiquark propagation. The differential cross section for $^{13}C(\gamma,\pi^+)^{13}B$ has also been calculated.

I. INTRODUCTION

Restoration of the chiral symmetry in the MIT bag model induced rapid development of the chiral bag models. This may be one of the most significant achievements in the intermediate-energy physics. Successes of the chiral bag models in description of the baryon structures encourage analyses of various processes such as pion-nucleon scatterings, electron-nucleon scatterings, and so on.

A single-pion photoproduction can also be a good example for application of the model. Since the pion fields are involved in this process, the chiral symmetry is naturally expected to play an important role in derivation of the scattering amplitude.

The chiral bag Lagrangian is generally of nonlinear form with surface or volume interaction between pions and quarks.[1,2] However, it might be shown that the Lagrangian with surface interaction could be transformed into that with volume interaction by a unitary chiral rotation of the quark field.[3]

In practical purposes, these nonlinear Lagrangians are expanded in a series of $(f_\pi R)^{-1}$ where f_π is the pion decay constant and R is the bag radius. The amplitude obtained up to second order from the Lagrangian with volume interaction contains a contact term in addition to those involving intermediate fermion propagators, in contrast to the amplitude derived from the surface interaction Lagrangian. This fact is worthwhile to keep in mind.

Araki and Kamal[4] analyzed the pion photoproduction on the nucleon by the chiral bag model and obtained reasonable results. However, their analyses are incomplete in the sense that not only the t-channel pion-pole term but also pion field contributions are ignored. These are expected to make significant contributions to the processes under consideration, since it is already confirmed that t-channel is important in the single-pion production studied on the nucleon level,[5,6] and the pion field plays a key role in the nucleon electromagnetic form factors.[7] In their calculation, the antiquark contribution to the (γ,π) processes was not taken into account either. Importance of this contribution can be conjectured from the fact that the antinucleon propagation played significant roles in the scattering amplitude derived on the nucleon level.[6]

In the present paper, we analyze the pion photoproduction on a nucleon by taking into account the t-channel pion-pole term, pion field contribution, and the antiquark diagram on the basis of the KE chiral bag model. Our calculations will be carried out in the static limit, and later we will improve it by taking a phase-space factor into account. We also extend our calculation to the process $^{13}C(\gamma,\pi^+)^{13}B$ at $E_\gamma=193$ MeV.

II. THEORY

A. Interaction Lagrangians

Starting from the chiral-invariant Lagrangian with σ field,[8] one can derive the effective Lagrangian of KE model[2] by the chiral transformations. In this model, the pion-quark interaction is given in the pseudovector coupling as

$$\mathcal{L}_{\pi qq}=\frac{1}{2f}\sum_a \bar{q}_a\gamma^\mu\gamma_5\boldsymbol{\tau}\cdot\partial_\mu\boldsymbol{\pi}q_a\theta_v \ , \tag{1}$$

where θ_v is the volume step function and f is the pion decay constant. The matrix element of $\mathcal{L}_{\pi qq}$ with $\langle\pi_a(\mathbf{k}_\pi), N(\mathbf{p}'\simeq 0)|$ and $|N(\mathbf{p}\simeq 0)\rangle$ gives the πNN interaction

$$\tilde{\mathcal{L}}_{\pi NN'}=-i\frac{g_{\pi NN'}(k_\pi)}{2M_N}\langle N'|\boldsymbol{\sigma}\cdot\mathbf{k}_\pi\tau^i|N\rangle \times(a_i-a_i^\dagger)2\pi\delta(E_{N'}-E_N-\omega_\pi) \ , \tag{2}$$

where $a_i^\dagger(a_i)$ is the pion creation (annihilation) operator, E_N and ω_π are the nucleon and pion energies, and the πNN form factor due to the bag volume $g_{\pi NN'}$ is[4]

$$g_{\pi NN'}(k_\pi)/2M_N=\frac{5}{6f}[K_0(k_\pi;j_0^2-\tfrac{1}{3}j_1^2)-\tfrac{4}{3}K_2(k_\pi;j_1^2)] \ , \tag{3}$$

with

$$K_l(k_\pi,F)\equiv\omega[2R^3(\omega-1)j_0^2(\omega)]^{-1} \times\int_0^R r^2dr\, j_l(k_\pi r)F\left[\frac{\omega}{R}r\right] . \tag{4}$$

Here, $\omega=2.0428$ is obtained by the bag boundary condition, $j_0(\omega)=j_1(\omega)$. The form factor $g_{\pi NN'}(k_\pi)$ given in Eq. (3) is associated with the lowest-order diagram shown in Fig. 1. Substituting the experimental value of the pion

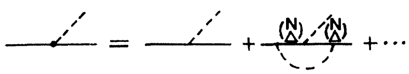

FIG. 1. Diagrams for renormalization of the πNN coupling constant.

decay constant $f=93$ MeV, we find the bare πNN coupling constant $[g_{\pi NN}(0)]^2/4\pi=9.58$. The renormalized πNN coupling constant $[g_{\pi NN}(0)]^2/4\pi=14.35$, which implies $f\simeq 76$ MeV, might be obtained by evaluating the higher-order diagrams. In this paper we take a conceivable way to obtain the dressed πNN form factor by using the value $f=76$ MeV in Eq. (3) and multiplying a monopole-type factor[9]

$$f_{\pi NB}(k_\pi)=\frac{\Lambda_B^2-m_\pi^2}{\Lambda_B^2-m_\pi^2+\mathbf{k}_\pi^2}\ , \tag{5}$$

with $\Lambda_N=8m_\pi$ and $\Lambda_\Delta=6m_\pi$, which was evaluated in the baryon space. Thus, $g_{\pi NN'}(k_\pi)$ in Eq. (2) is replaced by

$$\tilde{g}_{\pi NN'}(k_\pi)=g_{\pi NN'}(k_\pi)f_{\pi NN'}(k_\pi)\ . \tag{6}$$

Similarly, one can easily derive the $\pi N\Delta$ coupling Lagrangian by replacing $g_{\pi NN'}$, $\boldsymbol{\sigma}$, and τ^i in Eq. (2) by $\tilde{g}_{\pi N\Delta}$, $\mathbf{S}$, and T^i:

$$\mathcal{L}_{\pi N\Delta}=-i\frac{\tilde{g}_{\pi N\Delta}(k_\pi)}{2M_N}\langle \Delta|\mathbf{S}\cdot\mathbf{k}_\pi T^i|N\rangle \times(a_i-a_i^\dagger)2\pi\delta(E_\Delta-E_N-\omega_\pi)\ , \tag{7}$$

where $\mathbf{S}$ and T^i are the transition spin and isospin operators.[10] By SU(6) symmetry, we have

$$g_{\pi N\Delta}(k_\pi)=\frac{6\sqrt{2}}{5}g_{\pi NN}(k_\pi)\ , \tag{8}$$

and, then,

$$\tilde{g}_{\pi N\Delta}(k_\pi)=g_{\pi N\Delta}(k_\pi)f_{\pi N\Delta}(k_\pi)\ . \tag{8a}$$

The photon-quark coupling is generated by introducing the minimal substitution $\partial_\mu\rightarrow\partial_\mu+ieA_\mu$ as

$$\mathcal{L}_{\gamma qq}=-e_q\bar{q}_a\gamma^\mu A_\mu q_a\ , \tag{9}$$

$$\mathcal{L}_{\gamma\pi\pi}=ie[\pi^+(\partial^\mu\pi)-(\partial^\mu\pi^+)\pi]A_\mu\ , \tag{10}$$

$$\mathcal{L}_{\gamma\pi qq}=\frac{ie}{2f}\bar{q}_a\gamma^\mu A_\mu\gamma_5(\tau^-\pi^+-\tau^+\pi^-)q_a\ , \tag{11}$$

where e_q is the quark charge. The Lagrangian (9) can be converted into the baryonic bag space in the forms

$$\mathcal{L}_{\pi NN'}=ie\frac{G_M^N(k_\gamma)}{2M_N}\langle N'|\boldsymbol{\sigma}\cdot\mathbf{k}_\gamma x\hat{\varepsilon}|N\rangle \times 2\pi\delta(E_{N'}-E_N-\omega_\gamma)\ , \tag{12}$$

$$\mathcal{L}_{\gamma N\Delta}=ie\frac{G_M^\Delta(k_\gamma)}{2M_N}\langle \Delta|\mathbf{S}\cdot(\mathbf{k}_\gamma x\hat{\varepsilon})T_3|N\rangle \times 2\pi\delta(E_\Delta-E_N-\omega_\gamma)\ , \tag{13}$$

where $\mathbf{k}_\gamma$ and ω_γ are the photon momentum and energy, $\hat{\varepsilon}$ is the polarization vector, and

$$G_M^{N(\Delta)}(k_\gamma)=\sum_{j=1}^{3}G_j^{N(\Delta)}(k_\gamma)\ ,\qquad \frac{G_1^B(k_\gamma)}{2M_N}=a^B 2k_\gamma^{-1}K_1(k_\gamma;j_0j_1)\ , \tag{14}$$

$$\frac{G_2^B(k_\gamma)}{2M_N}=\sum_{S,S'=N,\Delta}\frac{1}{90\pi^2M_N^2k_\gamma}\left[\frac{1}{2f}\right]^2\int_0^\infty dk\, k^4\frac{\tilde{g}_{\pi NN'}^2(k)}{\omega_k}\frac{b_{ss'}^BK_1(k_\gamma;j_0j_1)}{(E_N-M_s-\omega_k)(E_B-M_{s'}-\omega_k)}\ , \tag{15}$$

$$\frac{G_3^B(k_\gamma)}{2M_N}=\sum_{S=N,\Delta}\frac{f_{\gamma\pi}(k_\gamma)}{16\pi^2M_N^2k_\gamma}\int_0^\infty\frac{dk\,dk'k^3k'^3\tilde{g}_{\pi NN'}(k')\tilde{g}_{\pi NN'}(k)}{\omega_k\omega_{k'}}C_S^BJ_S^B\int_0^\infty dr\, rj_1(k'r)j_1(kr)j_1(k_\gamma r)\ . \tag{16}$$

The form factors due to the quark bag volume $G_j^B(k_\gamma)$ are associated with the diagrams shown in Fig. 2. The previous work[4] did not take into account the contributions of pion cloud, i.e., $G_2^B(k_\gamma)$ and $G_3^B(k_\gamma)$, which play important roles in baryon electromagnetic form factors. We have introduced the $\gamma\pi$ form factor of a familiar type

$$f_{\gamma\pi}(k_\gamma)=(1+k_\gamma^2/m_\rho^2)^{-1}$$

in Eq. (16), where m_ρ is the mass of rho meson. The coefficients a^B, $b_{ss'}^B$, and c_s^B are given in real numbers as

$$a^p=-(\tfrac{3}{2})a^n=1\ ,$$

$$b_{NN}^p=-(\tfrac{1}{4})b_{NN}^n=\tfrac{5}{4}\ ,$$

$$b_{\Delta N}^p=b_{N\Delta}^p=-b_{N\Delta}^n=-b_{\Delta N}^n=16\ ,$$

$$b_{\Delta\Delta}^p=-4b_{\Delta\Delta}^n=32\ ,$$

$$c_N^p=-c_N^n=(\tfrac{25}{8})c_\Delta^p=-(\tfrac{25}{8})c_\Delta^n=2$$

for the nucleon, and

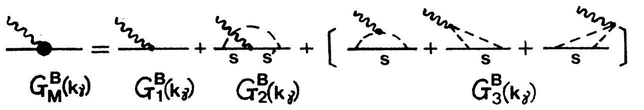

FIG. 2. Feynman diagrams for γNN vertex.

$$a^{\Delta}=1\ ,$$
$$b^{\Delta}_{NN}=b^{\Delta}_{\Delta\Delta}=\tfrac{4}{5}b^{\Delta}_{N\Delta}=(\tfrac{25}{2})b^{\Delta}_{\Delta N}=15\ ,$$
$$c^{\Delta}_{\Delta}=5c^{\Delta}_{N}=-\sqrt{2}$$

for Δ^+ and Δ^0. The propagator J^B_S is

$$J^B_S=[(E_N-M_S-\omega_k)(E_B-M_S-\omega_{k'})]^{-1}+[(\omega_\gamma-\omega_k-\omega_{k'})(E_B-\omega_{k'}-M_S)]^{-1}+[(E_N-\omega_k-M_S)(-\omega_k-\omega_{k'}-\omega_\gamma)]^{-1}\ . \qquad (17)$$

Similarly, the seagull term can be expressed in the baryonic bag space as follows:

$$\tilde{\mathcal{L}}_{\gamma NN'\pi}=-ie[g^{(1)}_{\pi\gamma}(\mathbf{k}_{\gamma\pi})\langle N'|\boldsymbol{\sigma}\cdot\hat{\varepsilon}\tau^i|N\rangle-2g^{(2)}_{\pi\gamma}(k_{\gamma\pi})\langle N'|(\boldsymbol{\sigma}\cdot\mathbf{k}_{\gamma\pi})(\hat{\varepsilon}\cdot\mathbf{k}_\pi)\tau^i|N\rangle\times 2\pi\delta(E_{N'}+\omega_\pi-E_N-\omega_\gamma)]\ , \qquad (18)$$

where $\mathbf{k}_{\gamma\pi}=\mathbf{k}_\gamma-\mathbf{k}_\pi$ and

$$g^{(1)}_{\gamma\pi}(k_{\gamma\pi})=\frac{5}{6f}[K_0(k_{\gamma\pi};j_0^2-\tfrac{1}{3}j_1^2)+\tfrac{2}{3}K_2(k_{\gamma\pi};j_1^2)]\ , \qquad (19)$$

$$g^{(2)}_{\gamma\pi}(k_{\gamma\pi})=\frac{5}{6f}K_2(k_{\gamma\pi};j_1^2)\ . \qquad (20)$$

The second term in Eq. (18) is very small compared with the first term and, then, we neglect it in the actual numerical calculations.

B. Antiquark contribution

The wave function of the 1s-state antiquark is given as[11]

$$\bar{q}=\left[\frac{\omega}{8\pi R^3(\omega-1)j_0^2(\omega)}\right]^{1/2}\times\begin{bmatrix} j_1[-(\omega/R)r]\boldsymbol{\sigma}\cdot\hat{r}\\ ij_0[-(\omega/R)r]\end{bmatrix}\chi_m\theta_v(r-R)\ . \qquad (21)$$

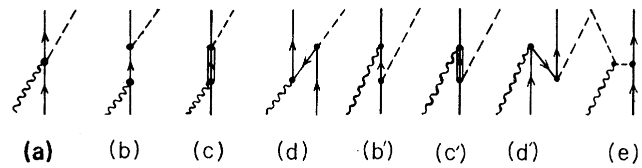

FIG. 3. Feynman diagrams for the pion photoproduction. (a) is the Seagull term. The s-channel diagrams (b) and (c) are corresponding to the processes in which the intermediate state baryons are nucleon and Δ particle, respectively. The diagram (d) shows the antiquark propagation in the s channel. The u-channel diagrams are given in (b′), (c′), and (d′), and the t channel is shown in (e).

The $\gamma q\bar{q}$ and $\pi\bar{q}q$ interaction Lagrangians in momentum space are expressed in the forms

$$\mathcal{L}_{\gamma q\bar{q}}(k_\gamma)=-f^{(1)}(k_\gamma)b'^{\dagger}_\alpha e_q(\boldsymbol{\sigma}\cdot\hat{\varepsilon})b_\alpha 2\pi\delta(\omega_{\bar{q}}-\omega_q-\omega_\gamma)\ , \qquad (22)$$

$$\mathcal{L}_{\pi\bar{q}q}(k_\pi)=-i\,f^{(2)}(k_\pi)b^\dagger_\alpha\boldsymbol{\tau}\cdot\boldsymbol{\pi}b'_\alpha 2\pi\delta(\omega_q-\omega_{\bar{q}}+\omega_\pi)\ , \qquad (23)$$

where $b'^{\dagger}(b^\dagger)$ and $b'(b)$ are antiquark (quark) creation and annihilation operators, $\omega_q=\omega/R$ and $\omega_{\bar{q}}=-\omega/R$ are the quark and antiquark energies, and

$$f^{(1)}(k_\gamma)=\omega_\pi[K_0(k_\gamma;j_0^2-\tfrac{1}{3}j_1^2)+\tfrac{2}{3}K_2(k_\gamma;j_1^2)]\ , \qquad (24)$$

$$f^{(2)}(k_\pi)=\frac{1}{2f}K_0(k_\pi;j_0^2+j_1^2)\ . \qquad (25)$$

C. Transition amplitudes

Making use of the interaction Lagrangian, one can derive the transition amplitudes for the pion photoproduction on a single nucleon. The contribution of the pion-pole term [Fig. 3(e)] can be calculated from the Lagrangian (10). Then, separating the transition amplitude into seagull term [Fig. 3(a)] from the Born term [Figs. 3(b), 3(c), 3(b′), 3(c′), and 3(e)], we find

$$T^{SG}_{\gamma\pi^\pm}=\pm i\sqrt{2}e\frac{g^{(1)}_{\gamma\pi}(k_{\gamma\pi})}{2M_N}\langle\chi_f|\boldsymbol{\sigma}\cdot\hat{\varepsilon}|\chi_i\rangle\ , \qquad (26)$$

$$T^B_{\gamma\pi^\pm}=-\sqrt{2}e\frac{\tilde{g}_{\pi NN}(k_\pi)}{2M_N}\langle\chi_f|\frac{(\boldsymbol{\sigma}\cdot\mathbf{k}_\pi)(\boldsymbol{\sigma}\cdot\mathbf{k}_\gamma\times\hat{\varepsilon})}{E_N-M_N+\omega_\pi}\frac{G^{\pm}_M(k_\gamma)}{2M_N}+\frac{(\boldsymbol{\sigma}\cdot\mathbf{k}_\gamma\times\hat{\varepsilon})(\boldsymbol{\sigma}\cdot\mathbf{k}_\pi)}{E_N-M_N-\omega_\pi}\frac{G^{\mp}_M(k_\gamma)}{2M_N}|\chi_i\rangle\pm i2\sqrt{2e}\frac{\tilde{g}_{\pi NN}(k_{\gamma\pi})}{2M_N}f_{\gamma\pi}(k_\gamma)\langle\chi_f|\frac{(\mathbf{k}_\pi\cdot\hat{\varepsilon})(\boldsymbol{\sigma}\cdot\mathbf{k}_{\gamma\pi})}{k^2_{\gamma\pi}+m^2_\pi}|\chi_i\rangle\ . \qquad (27)$$

The antiquark contributions, Figs. 3(d) and (3d′), are obtained in the similar fashion as

$$T^{\rm ant}_{\gamma\pi^\pm}=-i\sqrt{2}ef^{(1)}(k_\gamma)f^{(2)}(k_\pi)\left[\frac{a^\mp}{(2\omega/R)-\omega_\pi}+\frac{a^\pm}{(2\omega/R)+\omega_\pi}\right]\cdot\langle\chi_f|\sigma\cdot\hat{\varepsilon}|\chi_i\rangle\ , \tag{28}$$

where the positive (negative) superscript of $G_M^\pm(k_\gamma)$ denotes the proton (neutron), $a^+=\frac{20}{9}$, and $a^-=-\frac{10}{9}$. We neglect here a small term corresponding to the second term in Eq. (18). This term appeared in F_4 in Eq. (3-17) of Ref. 4 and was proven to be negligible. Similarly, the Δ-pole contributions are given as

$$T^\Delta_{\gamma\pi}=\mp\frac{\sqrt{2}}{3}\frac{G_M^\Delta(k_\gamma)}{2M_N}\frac{g_{\pi N\Delta}(k_\pi)}{2M_N}\left[\frac{\langle\chi_f|\mathbf{S}\cdot\mathbf{k}_\pi|\Delta\rangle\langle\Delta|\mathbf{S}\cdot(\mathbf{k}_\gamma\times\hat{\varepsilon})|\chi_i\rangle}{E_N-M_\Delta+\omega_\pi}+\frac{\langle\chi_f|\mathbf{S}\cdot(\mathbf{k}_\gamma\times\hat{\varepsilon})|\Delta\rangle\langle\Delta|\mathbf{S}\cdot\mathbf{k}_\pi|\chi_i\rangle}{E_N-M_\Delta-\omega_\pi}\right]. \tag{29}$$

By using the formulas for the Hermitian vectors **A** and **B**,

$$(\sigma\cdot\mathbf{A})^\dagger(\sigma\cdot\mathbf{B})=(\mathbf{A}\cdot\mathbf{B})+i\sigma\cdot(\mathbf{A}\times\mathbf{B})\ , \tag{30}$$

$$(\mathbf{S}\cdot\mathbf{A})^\dagger(\mathbf{S}\cdot\mathbf{B})=\tfrac{2}{3}(\mathbf{A}\cdot\mathbf{B})-\frac{i}{3}\sigma\cdot(\mathbf{A}\times\mathbf{B})\ , \tag{31}$$

these expressions are rewritten in the more practical forms

$$T_{\gamma\pi^\pm}=c_1(\sigma\cdot\hat{\varepsilon})+c_2\mathbf{k}_\pi\cdot(\mathbf{k}_\gamma\times\hat{\varepsilon})+c_3(\sigma\cdot\hat{\varepsilon})(\mathbf{k}_\pi\cdot\mathbf{k}_\gamma)+c_4(\sigma\cdot\mathbf{k}_\gamma)(\mathbf{k}_\pi\cdot\hat{\varepsilon})+c_5\frac{(\sigma\cdot\mathbf{k}_{\gamma\pi})(\mathbf{k}_\pi\cdot\hat{\varepsilon})}{\mathbf{k}^2_{\gamma\pi}+m^2_\pi}\ . \tag{32}$$

The coefficients are given as

$$C_1=i\sqrt{2}\left[\pm\frac{g^{(1)}_{\gamma\pi}(k_{\gamma\pi})}{2M_N}\left[1+\frac{\omega_\pi}{M_N}\right]^{-1}-f^{(1)}(k_\gamma)f^{(2)}(k_\pi)\left[\frac{a^\mp}{(2\omega/R)-\omega_\pi}+\frac{a^\pm}{(2\omega/R)+\omega_\pi}\right]\right], \tag{33}$$

$$C_2=\mp\xi^-(k_\gamma,k_\pi)\mp2\eta^-(k_\gamma,k_\pi)\ , \tag{34}$$

$$C_3=+i\xi^+(k_\gamma,k_\pi)\mp i\eta^+(k_\gamma,k_\pi)\ , \tag{35}$$

$$C_4=-i\xi^+(k_\gamma,k_\pi)\pm i\eta^+(k_\gamma,k_\pi)\ , \tag{36}$$

$$C_5=\pm i2\sqrt{2}e\frac{g_{\pi NN}(k_{\gamma\pi})}{2M_N}f_{\gamma\pi}(k_\gamma)\left[1+\frac{\omega_\pi}{M_N}\right]^{-1}, \tag{37}$$

where

$$\xi^\pm(k_\gamma,k_\pi)=\sqrt{2}e\frac{g_{\pi NN}(k_\pi)}{2M_N}\frac{1}{2M_N\omega_\pi}[G_M^+(k_\gamma)\pm G_M^-(k_\gamma)]\ , \tag{38}$$

$$\eta^\pm(k_\gamma,k_\pi)=\frac{\sqrt{2}}{9}e\frac{g_{\pi N\Delta}(k_\pi)}{2M_N}\left[\frac{1}{\omega_{\Delta N}-\omega_\pi}\pm\frac{1}{\omega_{\Delta N}+\omega_\pi}\right]\frac{G_M^\Delta(k_\gamma)}{2M_N}\ , \tag{39}$$

with $\omega_{\Delta N}=M_\Delta-M_N$. In order to improve the static limit, we have inserted a phase-space factor $(1+\omega_\pi/M_N)^{-1}$ in Eqs. (33) and (37). This factor is considered to yield approximately the first-order nucleon recoil effects.[5] Notice that all the coefficients C_j are determined by the bag radius R. On the other hand, the corresponding coefficients in the CGLN amplitude[5] are expressed with the phase shifts of π-N scattering.[5,12] And these phase shifts should be determined by analyzing the π-N scattering. The pion photoproduction amplitude derived in the present work contains only one free parameter, i.e., the bag radius R which is in the range of 0.6–1.0 fm.

III. RESULTS AND DISCUSSION

The differential cross sections for the pion photoproduction by the nucleon can easily be obtained with the transition amplitudes derived in the preceding section. Our results are shown in Figs. 4 and 5. Although our calculations contain only one free parameter, the bag radius R for which we used $R=0.8$ fm, excellent agreements with the measured cross sections have been obtained. The shape differences between (γ,π^+) and (γ,π^-) cross sections[13,14] are arising from the form factor $G_M^\pm(k_\gamma)$ and the antiquark propagation. Particularly important are the contributions of $G_2^B(k_\gamma)$ and $G_3^B(k_\gamma)$, Eqs. (15) and (16), which describe the pion cloud effects. These effects were completely ignored in the previous calculations.[4] In Fig. 6 we show the features of contributions from each term. The solid curve is the result obtained with all contributions considered in the present work. The dot-dashed curve has been calculated without the πNB form factors. The figure shows that these form factors are important to suppress the cross section so as to fit the data

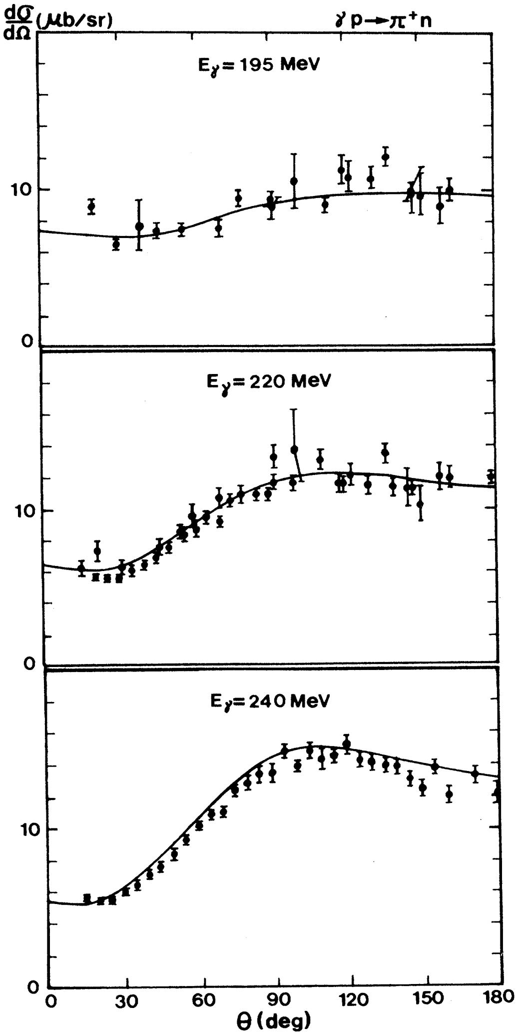

FIG. 4. The differential cross sections for $\gamma+p\rightarrow n+\pi^+$. The experimental results are taken from Ref. 13.

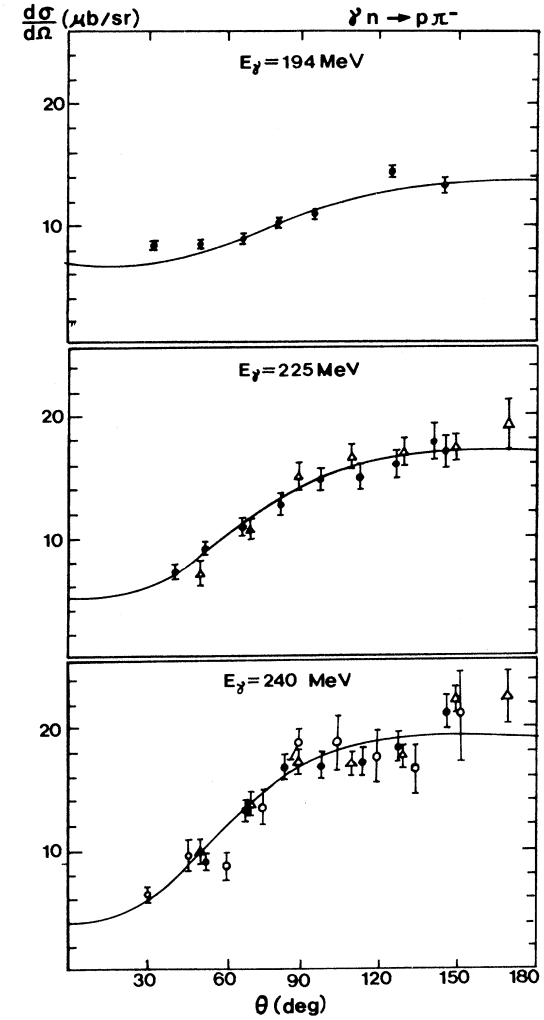

FIG. 5. The differential cross sections for $\gamma+n\rightarrow p+\pi^-$. The experimental results are taken from Ref. 14.

over all angles. When the pion-pole term is ignored, we obtain the dashed curve which shows disagreement with the data at smaller angles. The dotted curve corresponds to the result without the pionic effects, diagrams with pion propagations in Fig. 2. Obvious is the importance of pionic effects in the pion photoproduction. This is consistent with the fact that the pion field plays a conclusive role in the nucleon electromagnetic form factors, particularly the neutron electric form factors.[6,7,15] Although we do not show quantitatively the Δ contributions in this figure, Δ particles in the intermediate states of the processes play important roles to reproduce the experimental results. Even the shapes of the differential cross section cannot properly be reproduced without the Δ particles. We also find that the antiquark propagation plays a role to suppress the $\gamma\pi^+$ cross sections as much as 8% and enhance the $\gamma\pi^-$ cross sections as much as 18%.

The dot-dot-dashed curve in Fig. 6 shows the result calculated by neglecting both pionic effects and the pion-pole term. This curve is indeed the result obtained only with the diagrams proposed in the previous work.[4]

An application of the scattering amplitude, Eq. (32), to the pion photoproduction on nuclei is also possible. At low energies below the Δ resonance, one may expect that quarks are confined in the chiral bag which is well separated from the other bag in the nucleus. Namely, quarks are confined into nucleon and Δ particle and never exchanged between two baryons. Then, one can make use of the conventional nuclear wave functions to analyze the process. In Fig. 7, we expose our results for ^{13}C (γ,π^+) ^{13}B. We have used the Cohen-Kurath wave functions[16] for the nuclei, and the local Laplacian optical potential[17] has been applied to obtain the pion distorted wave. All effects considered here have been included to obtain the theoretical curves.

The dashed curve calculated with the "adjusted" pion

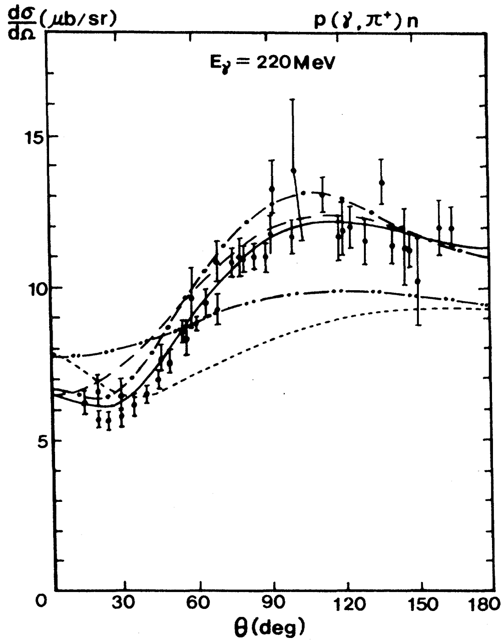

FIG. 6. The differential cross section for $\gamma+p\to n+\pi^+$ at $E_\gamma=220$ MeV. The solid curve has been obtained with all effects considered here. The dot-dashed or dashed curves are the results obtained by ignoring the πNB form factors $f_{\pi NB}(k_\pi)$ or the pion-pole term, respectively. The dotted curve corresponds to the calculation without the pionic effects. The dot-dot-dashed curve is obtained by neglecting both pionic effects and the pion-pole term. The data were taken from Ref. 13.

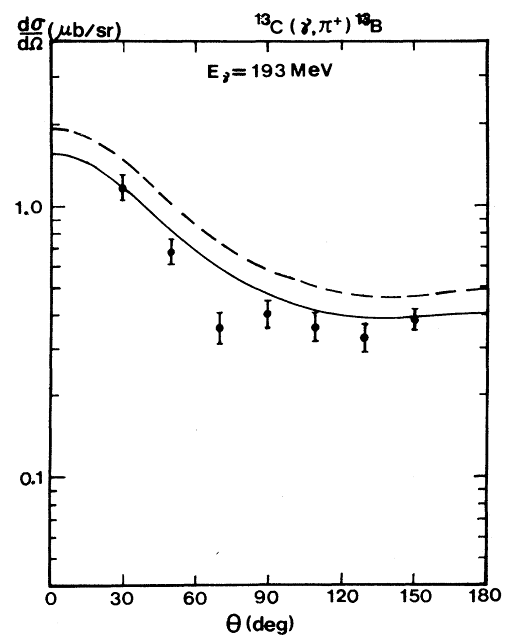

FIG. 7. The differential cross section for $^{13}C(\gamma,\pi^+)^{13}B$. The solid and dashed curves have been calculated with the renormalized πNN coupling constants associated with $f=83$ MeV and 76 MeV, respectively.

decay constant $f=76$ MeV is higher as much as 30% compared with the experimental results. The pion coupling to the nucleon inside the nucleus might be different from that to the free nucleon. The Δ particle-nucleon hole coupling could take place through the pion field in the nucleus, although it is absolutely absent in the free state of nucleon. This coupling gives rise to modify the πNN coupling constant in the nucleus as[18]

$$g^*_{\pi NN}(0)\simeq g_{\pi NN}(0)\left[1+\frac{\alpha/3}{1-\alpha/3}\right], \tag{40}$$

where $g_{\pi NN}(0)$ is the bare coupling constant obtained with $f=93$ MeV and the optical parameter α is given with the pion Compton wave length, the nuclear mass number A, and the nuclear radius $R_A=R_0A^{1/3}$ as[19]

$$\alpha=\frac{3A}{4\pi}\left[\frac{\lambda_\pi}{R_A}\right]^3. \tag{41}$$

For $R_0=1.25$ fm, we find $\alpha=0.335$ which induces $[g^*_{\pi NN}(0)]^2/4\pi=12.23$ corresponding to $f=83$ MeV. Use of this value yields the result shown by a solid curve in Fig. 7. Improvement is obvious.

IV. CONCLUSION

Our calculations based on the chiral bag model contain only one free parameter, i.e., the bag radius R, while the CGLN amplitude is given with the pion-nucleon scattering phase shifts which should be determined through analysis of the pion scattering by the nucleon. Nevertheless, the results are excellent. The secret of success is actually the point that we have taken into account the pion field effects, renormalization of the πNN coupling constants, t-channel contribution, and $\gamma\pi$, πNN, $\pi N\Delta$, $\pi\Delta\Delta$ form factors. All these contributions were neglected in the previous calculation.[4]

The antiquark propagations in intermediate states contribute significantly to the positive and negative pion photoproductions. This can be seen in the scattering amplitudes of $\pi^\pm$ photoproductions at threshold. Without antiquark propagations, we obtain

$$f(\gamma p\to n\pi^+)=-f(\gamma n\to p\pi^-)=0.0284m_\pi^{-1}$$

and $0.0286m_\pi^{-1}$ for $R=0.9$ fm and $R=0.8$ fm, respectively. Inclusion of the antiquark propagation gives

$$f(\gamma p\to n\pi^+)=0.0275m^{-1},$$
$$f(\gamma n\to p\pi^-)=-0.0315m_\pi^{-1}$$

for $R=0.9$ fm and

$$f(\gamma p\to n\pi^+)=0.0277m_\pi^{-1},$$
$$f(\gamma n\to p\pi^-)=-0.0314m_\pi^{-1}$$

for $R=0.8$ fm. The experimental data[20] are

$$f(\gamma p \to n\pi^+) = (0.0283 \pm 0.0005) m_\pi^{-1}$$

and

$$f(\gamma n \to p\pi^-) = (-0.0313 \pm 0.0020) m_\pi^{-1} .$$

Our results are in good agreement with the data.

The authors would like to express their gratitude to the Korea Science and Engineering Foundation for financial support.

[1]S. Théberge, A. W. Thomas, and G. A. Miller, Phys. Rev. D **22**, 2839 (1980).

[2]G. Kälbermann and J. M. Eisenberg, Phys. Rev. D **28**, 66 (1983).

[3]B. K. Jennings and O. V. Maxwell, Nucl. Phys. **A422**, 589 (1984).

[4]M. Araki and A. N. Kamal, Phys. Rev. D **29**, 1345 (1984).

[5]G. F. Chew, M. L. Goldberger, F. E. Low, and Y. Nambu, Phys. Rev. **106**, 1345 (1957).

[6]I. Blomqvist and J. M. Laget, Nucl. Phys. **A280**, 405 (1977).

[7]Y. J. Oh, K. J. Kong, and Il-T. Cheon, Phys. Rev. D **37**, 2570 (1988); S. Lee, K. J. Kong, and Il-T. Cheon, Phys. Lett. B **202**, 21 (1988).

[8]A. Chodos and C. B. Thorn, Phys. Rev. D **12**, 2733 (1975).

[9]M. Dillig and M. Brack, J. Phys. G **5**, 223 (1979).

[10]H. Sugawara and F. von Hippel, Phys. Rev. **172**, 1764 (1968).

[11]P. C. Hecking and G. F. Bertsch, Phys. Lett. **99B**, 237 (1981).

[12]Il-T. Cheon, Z. Phys. A **306**, 353 (1982).

[13]H. Genzel, P. Joos, and W. Pfeil, *Landolt-Börnstein Numerical Data and Functional Relationships in Science and Technology*, edited by K. H. Hellwege and A. M. Hellwege (Springer-Verlag, Berlin, 1973), Vol. 18.

[14]A. Bagheri, K. A. Aniol, F. Entezami, M. D. Hasinoff, D. F. Measday, J-M. Poutissou, M. Salomon, and B. C. Robertson, Phys. Rev. C **38**, 875 (1988).

[15]R. Tegen, R. Brockman, and W. Weise, Z. Phys. A **314**, 357 (1984).

[16]S. Cohen and D. Kurath, Nucl. Phys. **73**, 1 (1965).

[17]E. H. Auerbach, D. M. Fleming, and M. M. Sternheim, Phys. Rev. **162**, 1683 (1967).

[18]M. Ericson, A. Figureau, and C. Thévenet, Phys. Lett. **45B**, 19 (1973); K. Ohta and M. Wakamatsu, Phys. Lett. **51B**, 325 (1974).

[19]Il-T. Cheon, J. Korean Phys. Soc. **17**, 114 (1984).

[20]M. M. Lagels, J. J. De Swart, H. Nielsen, G. C. Oades, J. L. Petersen, B. Tromborg, G. Gustafson, A. C. Irving, C. Jarlskog, W. Pfeil, H. Pilkun, F. Steiner, and T. Tauscher, Nucl. Phys. **B109**, 1 (1976).